Rapid Reports

Correlating Ultrafast Function with Structure in Single Crystals of the Photosynthetic Reaction Center†

Libai Huang,‡,§ Gary P. Wiederrecht,§ Lisa M. Utschig,‡ Sandra L. Schlesselman,‡ Christina Xydis,||,⊥ Philip D. Laible,|| Deborah K. Hanson,|| and David M. Tiede*,‡

Chemical Sciences and Engineering Division, Center for Nanoscale Materials, and Biosciences Division, Argonne National Laboratory, Argonne, Illinois 60439-4831

Received June 12, 2008; Revised Manuscript Received July 30, 2008

ABSTRACT: Femtosecond transient absorbance spectroscopy was applied to the study of primary electron transfer in single reaction center crystals from *Rhodobacter sphaeroides*. Polarized transient absorption spectra of individual crystals are shown to correlate with polarized ground-state absorption spectra and to track cofactor transition moment directions calculated from the crystallographic structure. Electron transfer from the bacteriochlorophyll dimer to the bacteriopheophytin acceptor was found to be multiphasic in crystals and ~2-fold slower than in solution. This work demonstrates the ability to resolve ultrafast photosynthetic function in single crystals and allows ultrafast function to be directly correlated with structure.

Photosynthetic reaction centers (RCs)[1] are pigment−protein complexes that carry out the first light-induced chemical reactions in photosynthesis and serve as a paradigm for investigation of long-range electron transfer between noncovalently linked donors and acceptors. Crystal structures of bacterial photosynthetic RCs show two sets of bacteriochlorophyll (BChl), bacteriopheophytin (BPh), and quinone (Q) cofactors that are associated primarily with either the L- or M-protein subunits and are arranged in approximate 2-fold symmetry about the primary electron donor (P), composed of an exciton-coupled pair of BChls (*1*−*4*). However, the quantitative link between RC coordinate structure and photochemical function remains to be established because of the lack of time-resolved spectroscopic studies of photochemical function in crystals. For example, steady-state measurements of charge recombination kinetics from P^+Q^- charge-separated states in *Blastochloris viridis* RCs were found to differ in solution and crystalline samples, with crystals showing an additional slow, multisecond kinetic phase that is not seen in solution (*5*). Indistinguishable biphasic electron transfer between the reaction center quinones (Q_A and Q_B) was assessed in crystalline and solution states for the *Rhodobacter (Rb.) sphaeroides* RC (*6*), although other solution phase studies with *Rb. sphaeroides* differ by showing a faster kinetic phase on the microsecond time scale and the absence of a slow millisecond kinetic component (*7, 8*). Similarly, excited-state lifetimes of the chlorophyll cofactor in the cytochrome b_6f complex were found to be 3−6-fold longer in crystals than in solution (*9*). More generally, there is recognition of possible altered enzymatic function in crystalline states (*10, 11*). These considerations raise questions about how well the details of photosynthetic structure can be correlated to time-resolved function. Herein, we present the first femtosecond spectroscopy studies for single crystals of the RC from *Rb. sphaeroides*. Our results demonstrate a clear difference between crystal and solution-state time-resolved function and provide a direct measure of ultrafast photosynthetic electron transfer that can be linked to RC coordinate structure. Furthermore, these studies demonstrate unique opportunities to exploit the fixed orientation of cofactors within crystals to achieve site-specific resolution of photosynthetic function within cofactor manifolds.

Figure 1a shows polarized ground-state absorption spectra for a RC crystal from "wild-type" *Rb. sphaeroides* crystallized in the $P2_12_12_1$ unit cell and used for ultrafast experiments, measured with light polarized either parallel (0°) or perpendicular (90°) to the long axis of the needle-shaped crystal (inset in Figure 1a). Analyses of the optical absorption from single RC crystals have been made for the $P4_32_12$ crystals of *B. viridis* (*12*) but not from *Rb. sphaeroides*, although preliminary spectra have been reported (*13*). The polarized absorption spectra show pronounced changes in both absorption peak positions and amplitudes. Peak shifts are particularly significant since they reflect polarization-resolved contributions of individual transitions within the normally overlapping absorption bands of redundant cofactors in L- and M-protein subunits. Calculations based on crystal structures indicate that among the RC cofactors, the two BPhs have the weakest intercofactor coupling (*14*−*19*) and can be expected to have optical transitions aligned closest to the directions expected for an isolated bacteriochlorin.

† Supported by the U.S. DOE Office of Basic Energy Sciences under Contract DE-AC02-06CH11357.

* To whom correspondence should be addressed. E-mail: tiede@anl.gov. Phone: (630) 252-3539. Fax: (630) 252-9289.

‡ Chemical Sciences and Engineering Division.

§ Center for Nanoscale Materials.

|| Biosciences Division.

⊥ Consultant contracted through Lab Support, Rosemont, IL 60018.

[1] Abbreviations: BChl, bacteriochlorophyll; BPh, bacteriopheophytin; Q, quinone; P, special pair; RC, reaction center.

10.1021/bi801026g CCC: $40.75
Published on Web 10/11/2008

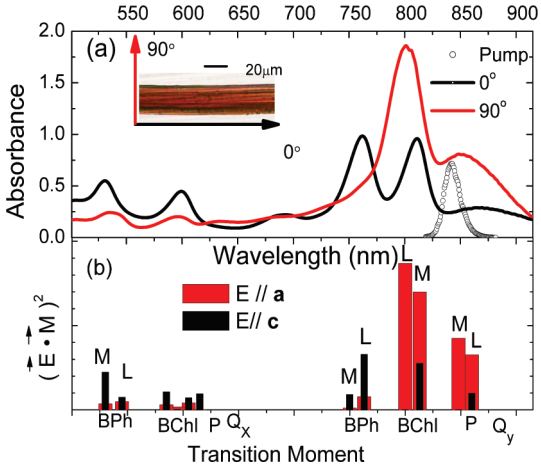

FIGURE 1: Polarized ground-state absorption spectra of a single photosynthetic reaction center crystal ($P2_12_12_1$) from *Rb. sphaeroides*. (a) Spectra with light polarized parallel (black line, 0°) and perpendicular (red line, 90°) to the long axis of the crystal. The laser pump spectrum is denoted with empty circles. The inset is a digital camera image of a typical crystal. (b) Extinction coefficient-weighted transition moment projections along *a* and *c* crystal axes.

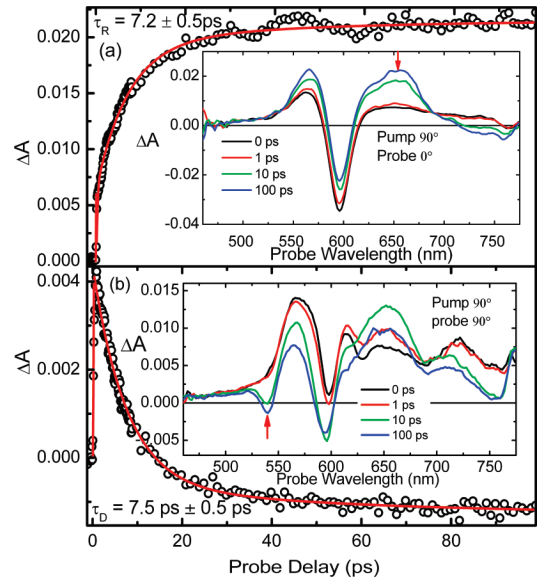

FIGURE 2: Transient absorption spectra (insets) and kinetics for a quinone-reduced RC crystal. Pump polarization was fixed at 90° and transients measured with the probe at 0° (a) and 90° (b) respectively. Red arrows in the insets mark the wavelengths for kinetics measurements. The red solid lines are biexponential fits convoluted with the pump pulse with fast component time constants indicated in the figure.

Therefore, we utilized the transitions of two BPhs near 540 nm (Q_x) and near 760 nm (Q_y) as references to identify the alignment of the coordinate unit cell axes with respect to the experimental measurements. Magnitudes for polarized optical absorption for the RC $P2_12_12_1$ unit cell were calculated from the transition moment, $\vec{m}$, and the polarized light electric field, $\vec{E}$, unit vectors as described in the Supporting Information. Extinction coefficient-weighted projections for each of the RC cofactor optical transitions, $\varepsilon(\vec{E}\ \vec{m})^2$, along *a* and *c* crystal axes are plotted with wavelength positions according to cofactor peak assignments (*20*−*22*) in Figure 1b. The alignment of the crystal unit cell axes with the experimental 0° and 90° directions was determined by the close agreement of the measured 0° and 90° polarized absorption patterns and the projection patterns calculated for the BPh Q_x and Q_y transition moments along the unit cell *c* and *a* axes, respectively.

The red-most absorption band arises from the lower energy exciton component of P (P_-) comprised of the exciton-coupled Q_y transitions for the two BChl molecules, P_L and P_M, that form P (*23*). The polarized spectrum recorded for P_- is found to have a strong preferential absorption with 90° polarized light. In addition, the polarized crystal spectra also showed a notable shift in the absorption peak position for P_- that changed from 850 nm in the spectrum recorded with 90° polarized light to 865 nm when measured with 0° polarized light. The polarization-dependent shift in the absorption peak for P_- is remarkable since it indicates that the absorption band is composed of a combination of transitions that are aligned with different projections along the crystal axes. Low-temperature (*24*−*27*) and hole burning (*27, 28*) spectroscopic measurements have demonstrated the presence of a low-energy shoulder on the P_- absorption band which has been identified as a (0-0) vibronic transition followed by a progression of higher-energy vibronic transitions that comprise the main absorption of P_- (*27, 28*). We note that absorption spectra of pyrochlorophyllide *a* in apomyoglobin single crystals showed polarization-dependent Q_y absorption peak shifts due to differences in the coupling of the Q_y vibronic levels with Q_x transitions (*29*). We suggest that the polarization-dependent shifts in the absorption observed for P_- in RC crystals could similarly reflect the vibronic structure of P_-.

Primary charge separation processes in quinone-reduced single crystals were investigated by femtosecond pump−probe spectroscopy. For comparison, charge separation processes were also assessed for quinone-reduced RCs in solution, and the results are presented in Figure S3 of the Supporting Information. The excitation wavelength was tuned to 844 nm as shown in Figure 1, which excites primarily the P_- transition. Transient measurements are shown with the probe polarization in the 0° (Figure 2a) and 90° (Figure 2b) directions and with the pump polarization fixed at 90°. Companion measurements with the pump polarization at 0° are shown in Figure S4 of the Supporting Information. The transient spectra show strong probe polarization dependencies. The crystal transient absorption spectra (insets in Figure 2) display a bleach of Q_x ground-state absorption of P at 595 nm as well as growth of the BPh^- anion band at 650−670 nm for both probe polarizations. However, bleaching of the Q_x transition of BPh around 540 nm is seen exclusively with the 90° polarized probe (inset in Figure 2b). This observation is consistent with experimental polarized ground-state spectra, and differences with the calculated projections demonstrate that the BPh_L Q_x transition moment is shifted from the assumed molecular position.

Transient spectra at early delay times also exhibit pronounced dichroism. With 90° probe polarization, a raised baseline and various absorption bands from 500 to 750 nm are noticeable for the 0 and 1 ps transient absorption spectra, compared to the mostly flat baseline, detected with 0° probe polarization. Transient features at early times are related to the P* excited state, and this strong dichroism implies that the transition dipole of P* aligns preferentially along the *c*

axis of the crystal. A similar dependence of probe polarization was also observed for pump polarization parallel (0°) to the long axis (Figure S4 of the Supporting Information). These results demonstrate the capability of isolating a single transition among the cofactor manifold by using polarized light to both pump and probe along fixed directions in the RC and provide the opportunity to directly correlate function to coordinate structures. Other polarization selection techniques such as pump−probe anisotropy measurements in solution (*22, 23, 25*) and linear dichroism with mechanically aligned samples (*21, 24*) provide only one-dimensional ordering that cannot be directly related to crystal structure.

The kinetics of the bleach of the BPh Q_x band was fit with a biexponential decay with 7.5 ± 0.5 ps (85%) and 56.7 ± 2.0 ps (15%) time constants (Figure 2b) and the growth of the BPh^- anion band fit with biexponential rise times of 7.2 ± 0.5 ps (90%) and 40 ± 2.0 ps (10%) (Figure 2a), indicating that the time for transfer of an electron from P* BPh, is heterogeneous, with an ∼7 ps transfer time for the fast component in this RC crystal. Both the fast and slow kinetic phases of the P* to BPh electron transfer are found to be approximately 2-fold slower than the corresponding phase measured in solution (Figure S3 of the Supporting Information). Detection wavelength-dependent kinetics (*30*) and biexponential emission decay kinetics from P* (*31*−*33*) have previously been discussed to arise from a conformational heterogeneity in the RC. The results presented here demonstrate that the conformational heterogeneity persists in crystals and must be contained within the thermal factors for X-ray coordinate data. The kinetic deceleration appears to uniformly affect both kinetic phases, suggesting a common, possibly energetic origin.

The ground-state dichroism shows that the pump polarization can be used in single-crystal studies to selectively excite otherwise degenerate optical transitions. For a fixed probe polarization of 90°, transient spectra corresponding to a pump polarization of 90° or 0° are shown in Figure 2b and Figure S4b, respectively. Comparable transient spectra are observed for the two pump polarizations at 844 nm, indicating that the same sequence of excited states is created when exciting within the different vibronic transitions of P. However, we have observed different transient states with the 800 nm pump, polarization-selective excitation of $BChl_L$ and $BChl_M$. These results will be reported elsewhere.

We have demonstrated the ability to carry out polarized femtosecond pump−probe spectroscopy on single RC crystals and have established a direct connection between ultrafast photosynthetic function and structure in the crystalline state. This approach offers opportunities to resolve energy and electron transfer functions for selected cofactors within the bacterial RC as well as with more spectrally complex RC−light harvesting 1 and photosystem I and photosystem II single-crystal samples.

SUPPORTING INFORMATION AVAILABLE

Experimental methods for crystallization, ground-state and transient absorption spectroscopy, and calculations of transition moment projections. This material is available free of charge via the Internet at http://pubs.acs.org.

REFERENCES

1. Feher, G., Allen, J. P., Okamura, M. Y., and Rees, D. C. (1989) *Nature 339*, 111–116.
2. Yeates, T. O., Komiya, H., Chirino, A., Rees, D. C., Allen, J. P., and Feher, G. (1988) *Proc. Natl. Acad. Sci. U.S.A. 85*, 7993–7997.
3. Michel, H. (1982) *J. Mol. Biol. 158*, 567–572.
4. Chang, C.-H., El-Kabbani, O., Tiede, D. M., Norris, J., and Schiffer, M. (1991) *Biochemistry 30*, 5352–5360.
5. Baxter, R. H. G., Krausz, E., and Norris, J. R. (2006) *J. Phys. Chem. B 110*, 1026–1032.
6. Axelrod, H. L., Abresch, E. C., Paddock, M. L., Okamura, M. Y., and Feher, G. (2000) *Proc. Natl. Acad. Sci. U.S.A. 97*, 1542–1547.
7. Li, J. L., Gilroy, D., Tiede, D. M., and Gunner, M. R. (1998) *Biochemistry 37*, 2818–2829.
8. Tiede, D. M., Vazquez, J., Cordova, J., and Marone, P. A. (1996) *Biochemistry 35*, 10763–10775.
9. Dashdorj, N., Yamashita, E., Schaibley, J., Cramer, W. A., and Savikhin, S. (2007) *J. Phys. Chem. B 111*, 14405–14410.
10. Efremov, R., Gordeliy, V. I., Heberle, J., and Buldt, G. (2006) *Biophys. J. 91*, 1441–1451.
11. Kort, R., Ravelli, R. B., Schotte, F., Bourgeois, D., Crielaard, W., Hellingwerf, K. J., and Wulff, M. (2003) *Photochem. Photobiol. 78*, 131–137.
12. Knapp, E. W., Fischer, S. F., Zinth, W., Sander, M., Kaiser, W., Deisenhofer, J., and Michel, H. (1985) *Proc. Natl. Acad. Sci. U.S.A. 82*, 8463–8467.
13. Reiss-Husson, F., and Mäntele, W. (1988) *FEBS Lett. 239*, 78–82.
14. Warshel, A., and Parson, W. W. (1987) *J. Am. Chem. Soc. 109*, 6143–6152.
15. Parson, W. W., and Warshel, A. (1987) *J. Am. Chem. Soc. 109*, 6152–6163.
16. Thompson, M. A., and Zerner, M. C. (1991) *J. Am. Chem. Soc. 113*, 8210–8215.
17. Lathrop, E. J. P., and Friesner, R. A. (1994) *J. Phys. Chem. 98*, 3056–3066.
18. Zhou, H. L., and Boxer, S. G. (1997) *J. Phys. Chem. B 101*, 5759–5766.
19. Chang, C. H., Hayashi, M., Liang, K. K., Chang, R., and Lin, S. H. (2001) *J. Phys. Chem. B 105*, 1216–1224.
20. Straley, S. C., Parson, W. W., Mauzerall, D. C., and Clayton, R. K. (1973) *Biochim. Biophys. Acta 305*, 597–609.
21. Breton, J. (1985) *Biochim. Biophys. Acta 810*, 235–245.
22. Kirmaier, C., and Holten, D. (1987) *Photosynth. Res. 13*, 225–260.
23. Jonas, D. M., Lang, M. J., Nagasawa, Y., Joo, T., and Fleming, G. R. (1996) *J. Phys. Chem. 100*, 12660–12673.
24. Vermeglio, A., and Paillotin, G. (1982) *Biochim. Biophys. Acta 681*, 32–40.
25. Hoff, A. J., Denblanken, H. J., Vasmel, H., and Meiburg, R. F. (1985) *Biochim. Biophys. Acta 806*, 389–397.
26. Tang, D., Jankowiak, R., Gillie, J. K., Small, G. J., and Tiede, D. M. (1988) *J. Phys. Chem. 92*, 4012–4015.
27. Klevanik, A. V., Ganago, A. O., Shkuropatov, A. Y., and Shuvalov, V. A. (1988) *FEBS Lett. 237*, 61–64.
28. Johnson, S. G., Tang, D., Jankowiak, R., Hayes, J. M., Small, G. J., and Tiede, D. M. (1990) *J. Phys. Chem. 94*, 5849–5855.
29. Boxer, S. G., Kuki, A., Wright, K. A., Katz, B. A., and Xuong, N. H. (1982) *Proc. Natl. Acad. Sci. U.S.A. 79*, 1121–1125.
30. Kirmaier, C., and Holten, D. (1990) *Proc. Natl. Acad. Sci. U.S.A. 87*, 3552–3556.
31. Vos, M. H., Lambry, J. C., Robles, J. C., Youvan, D. C., Breton, J., and Martin, J.-L. (1991) *Proc. Natl. Acad. Sci. U.S.A. 88*, 8885–8889.
32. Du, M., Rosenthal, S. J., Xie, X., DiMagno, T. J., Schmidt, M., Hanson, D. K., Schiffer, M., Norris, J. R., and Fleming, G. R. (1992) *Proc. Natl. Acad. Sci. U.S.A. 89*, 8517–8521.
33. Peloquin, J. M., Lin, S., Taguchi, A. K. W., and Woodbury, N. W. (1995) *J. Phys. Chem. 99*, 1349–1356.

BI801026G